

Methodology for optimal sizing of stand-alone photovoltaic/wind-generator systems using genetic algorithms

Eftichios Koutroulis ^{a,*}, Dionissia Kolokotsa ^b,
Antonis Potirakis ^a, Kostas Kalaitzakis ^a

^a Department of Electronic and Computer Engineering, Technical University of Crete, GR-73100 Chania, Greece

^b Department of Natural Resources and Environment, Technological Educational Institute of Crete, GR-73133 Chania, Greece

Received 25 May 2005; received in revised form 4 November 2005; accepted 17 November 2005

Available online 27 December 2005

Communicated by: Associate Editor Mukund Patel

Abstract

A methodology for optimal sizing of stand-alone PV/WG systems is presented. The purpose of the proposed methodology is to suggest, among a list of commercially available system devices, the optimal number and type of units ensuring that the 20-year round total system cost is minimized subject to the constraint that the load energy requirements are completely covered, resulting in zero load rejection. The 20-year round total system cost is equal to the sum of the respective components capital and maintenance costs. The cost (objective) function minimization is implemented using genetic algorithms, which, compared to conventional optimization methods such as dynamic programming and gradient techniques, have the ability to attain the global optimum with relative computational simplicity. The proposed method has been applied for the design of a power generation system which supplies a residential household. The simulation results verify that hybrid PV/WG systems feature lower system cost compared to the cases where either exclusively WG or exclusively PV sources are used.

© 2005 Elsevier Ltd. All rights reserved.

Keywords: Photovoltaic power systems; Wind power generation; Genetic algorithms

1. Introduction

Photovoltaic (PV) and Wind Generator (WG) power sources are widely used in order to supply power to consumers in remote areas. Due to their almost complementary power production character-

istics, they are usually used in hybrid system configurations. The block diagram of a stand-alone hybrid PV/WG system is shown in Fig. 1. Battery chargers, connected to a common DC bus, are used to charge the battery bank from the respective PV and WG input power sources, which are usually configured in multiple power generation blocks according to the devices nominal power ratings and the redundancy requirements. Depending on the battery charger technology, the maximum available power can

* Corresponding author. Tel.: +30 28210 37233; fax: +30 28210 37542.

E-mail address: efkout@electronics.tuc.gr (E. Koutroulis).

Nomenclature

α_w	WG size (m ²)	n_2	conversion factor (%)
α_s	PV size (m ²)	N_{ch}^{PV}	number of PV battery chargers
c_w	WG cost per unit area (\$/m ²)	N_{PV}	total number of PV modules
c_s	PV cost per unit area (\$/m ²)	P_{ch}^m	power rating of the selected battery charger (W)
$d(t)$	average daily demand at day t (kW h)	P_{PV}^m	maximum power of one PV module under STC (W)
$W(t)$	WG energy production at day t per unit area (kW h/m ²)	h	WG installation height (m)
$S(t)$	PV energy production at day t per unit area (kW h/m ²)	h_{ref}	reference WG height (m)
N	number of PV modules	$P_{WG}^i(t, h)$	power transferred to the battery bank at hour t of day i , from a WG installed at height h (W)
N_b	number of batteries	$v^i(t, h)$	wind speed at height h (m/s)
α	PV module cost (\$)	$v_{ref}^i(t)$	reference wind speed measured at height h_{ref} (m/s)
b	battery cost (\$)	a	power law exponent
N_P	number of PV modules connected in parallel	C_n	battery bank total nominal capacity (A h)
N_S	number of PV modules connected in series	DOD	maximum permissible depth of discharge (%)
$P_M^i(t, \beta)$	maximum output power of the PV array on day i ($1 \leq i \leq 365$) and at hour t ($1 \leq t \leq 24$) (W)	C_{min}	minimum permissible battery capacity during discharging (A h)
$I_{SC}^i(t, \beta)$	PV module short-circuit current (A)	$C^i(t)$	available battery capacity at hour t of day i (A h)
$I_{SC,STC}$	PV module short-circuit current under STC (A)	n_B	battery efficiency (%)
β	PV module tilt angle (°)	V_{BUS}	DC bus voltage (V)
$G^i(t, \beta)$	global irradiance incident on the PV module placed at tilt angle β (W/m ²)	$P_B^i(t)$	battery input/output power (W)
K_I	short-circuit current temperature coefficient (A/°C)	Δt	simulation time step (h)
$V_{OC}^i(t)$	PV module open-circuit voltage (V)	n_B^S	number of batteries connected in series
$V_{OC,STC}$	open-circuit voltage under STC (V)	V_B	nominal voltage of each individual battery (V)
K_V	open-circuit voltage temperature coefficient (V/°C)	N_{BAT}	total number of batteries
$T_A^i(t)$	ambient temperature (°C)	C_B	nominal capacity of each battery (A h)
NCOT	Nominal Cell Operating Temperature (°C)	$P_{re}^i(t)$	total power transferred to the battery bank during day i and hour t (W)
$FF^i(t)$	Fill Factor	N_{WG}	total number of WGs
β_1	PV module tilt angle from January until April and September until December (°)	$P_L^i(t)$	DC/AC inverter input power (W)
β_2	PV module tilt angle for the rest of the year (°)	$P_{load}^i(t)$	power consumed by the load at hour t of day i (W)
V_{DC}^m	battery charger maximum input voltage (V)	n_i	DC/AC converter efficiency (%)
V_{OC}^m	PV modules maximum open-circuit voltage (V)	$J(\mathbf{x})$	20-year round total system cost function (€)
$P_{PV}^i(t, \beta)$	PV power transferred to the battery bank on day i (W)	$C_c(\mathbf{x})$	total capital cost function (€)
n_s	battery charger conversion factor	$C_m(\mathbf{x})$	maintenance cost function (€)
n_1	battery charger power electronic interface efficiency (%)	\mathbf{x}	vector of the decision variables
		h_{low}	WG tower lower height limit (m)
		h_{high}	WG tower upper height limit (m)
		C_{PV}	capital cost of one PV module (€)

C_{WG}	capital cost of one WG (€)	C_{INV}	capital cost of the DC/AC inverter (€)
C_{BAT}	capital cost of one battery (€)	y_{BAT}	expected number of battery replacements during the 20-year system operation
M_{PV}	maintenance cost per year of one PV module (€/year)	M_{ch}^{PV}	maintenance cost per year of one PV battery charger (€/year)
M_{WG}	maintenance cost per year of one WG (€/year)	M_{INV}	maintenance cost per year of one DC/AC inverter (€/year)
M_{BAT}	maintenance cost per year of one battery (€/year)	C_{max}	absolute minimum of function $J(x)$ calculated at each generation (€)
C_h	WG tower capital cost per meter (€/m)	p_{sc}	initial probability of Simple Crossover
C_{hm}	WG tower maintenance cost per meter and year (€/m/year)	p_{sac}	initial probability of Simple Arithmetical Crossover
C_{ch}^{PV}	capital cost of one PV battery charger (€)	p_{wac}	initial probability of Whole Arithmetical Crossover
y_{ch}^{PV}	expected number of PV battery charger replacements during the 20-year system lifetime	p_{um}	uniform mutation probability
y_{INV}	expected number of DC/AC inverter replacements during the 20-year system lifetime	p_{bm}	boundary mutation probability
		p_{num}	non-uniform mutation probability

be extracted from the PV and WG power sources (Maximum Power Point Tracking, MPPT), (Lorenzo, 1994; De Broe et al., 1999). The battery bank, which is usually of lead-acid type, is used to store the energy surplus and to supply the load in case of low wind speed and/or irradiation conditions. A DC/AC converter (inverter) is used to interface the DC battery voltage to the consumer load AC requirements. The outputs of all battery chargers, the battery bank and the DC/AC converter input

terminals are connected in parallel. The energy produced from each PV or WG source is transferred to the consumer load through the battery charger and the DC/AC inverter, while the energy surplus is used to charge the battery bank.

Because of the intermittent solar irradiation and wind speed characteristics, which highly influence the resulting energy production, the major aspects in the design of PV and WG power generation systems are the reliable power supply of the consumer

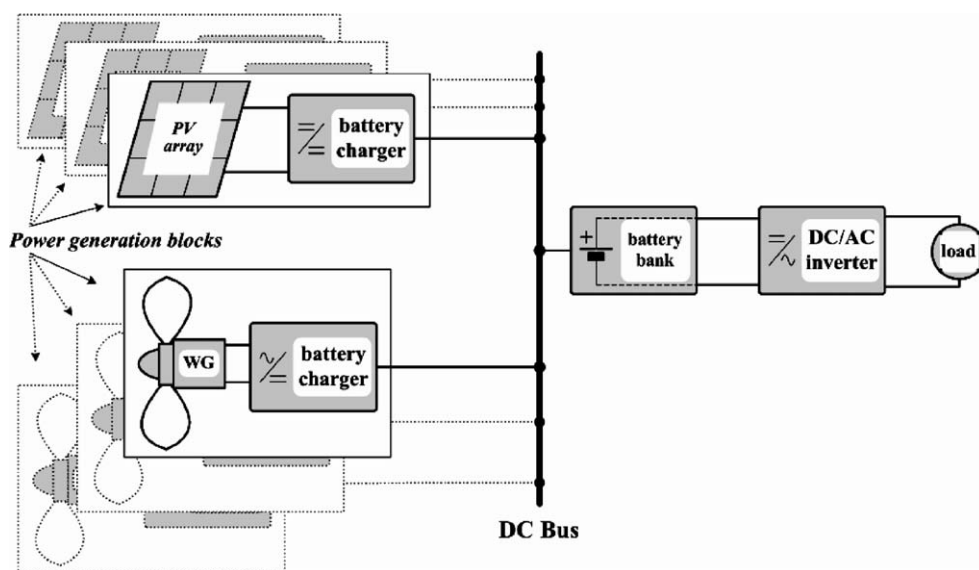


Fig. 1. Block diagram of a hybrid PV/WG system.

under varying atmospheric conditions and the corresponding total system cost. Considering the wide range of commercially available device types, it is essential to select the number and type of PV modules, WGs and batteries, and their installation details such that power is uninterruptedly supplied to the load and simultaneously the minimum system cost is achieved.

A sizing method of stand-alone PV systems has been presented by [Shrestha and Goel \(1998\)](#), which is based on energy generation simulation for various numbers of PVs and batteries using suitable models for the system devices (PVs, batteries, etc.). The selection of the numbers of PVs and batteries ensures that reliability indices such as the Loss of Load Hours (LOLH), the lost energy and the system cost are satisfied. In a similar method, Markov chain modeling is used for the solar radiation. In this case, the number of PVs and batteries are selected according to the desired System Performance Level (SPL) requirement, which is defined as the number of days that the load cannot be satisfied and it is expressed in terms of probability ([Maghraby et al., 2002](#)).

A design method for hybrid PV/WG systems, based on energy balance, has been proposed by [Kellogg et al. \(1998\)](#). Using the hourly average data of wind speed, solar radiation and consumer power demand, the difference of generated and demanded power (ΔP) is calculated over a 24-h period. The numbers of PV modules and WGs are finally selected, using an iterative procedure where the system operation is simulated for various numbers of PVs and WGs, such that ΔP has an average value of zero. The total annual cost for each configuration is calculated and the combination with the lowest cost is selected to represent the optimal mixture.

The seasonal variation of PV and WG power generation is taken into account in the method proposed by [Markvart \(1996\)](#), where the problem of optimal sizing the PV and WG power sources in a hybrid generation system is formulated as follows:

$$\text{minimize : system cost} = c_s \cdot \alpha_s + c_w \cdot \alpha_w \quad (1)$$

$$\text{subject to : } d(t) \leq W(t) \cdot \alpha_w + S(t) \cdot \alpha_s \quad (2)$$

where α_w and α_s are the WG and PV sizes (m^2), c_w and c_s represent the corresponding costs per unit area ($\$/\text{m}^2$), $d(t)$ is the average daily demand at day t (kW h) and $W(t)$, $S(t)$ are the WG and PV energy productions at day t per unit area ($\text{kW h}/\text{m}^2$), respectively.

Using the values of $d(t)$, $W(t)$ and $S(t)$ during the year, a plot of α_w versus α_s is obtained and the optimal configuration is defined on this curve as the point where

$$\frac{d\alpha_s}{d\alpha_w} = -\frac{c_w}{c_s} \quad (3)$$

However, using this method the battery size is not included in the optimization process.

A method for the selection of the optimum combination of battery and PV array in a hybrid PV/WG system has been presented by [Borowy and Salameh \(1996\)](#). The system operation is simulated for various combinations of PV array and battery sizes and the Loss of Power Supply Probability (LPSP) is calculated for each combination. Then, for the desired LPSP, the PV array versus battery size are plotted and the optimal solution, which minimizes the total system cost, is defined as the point on the sizing curve where

$$\frac{dN}{dN_b} = -\frac{b}{a} \quad (4)$$

where N , N_b are the number of PV modules and batteries and a , b are the costs (\$) of a PV module and a battery, respectively.

In a similar method ([Bagul et al., 1996](#)), the N versus N_b curve is plotted using a probabilistic analysis of the daily energy surplus. In both methods, the WG size is not included in the optimization process.

According to the methods proposed by [Chedid and Rahman \(1997\)](#) and [Yokoyama et al. \(1994\)](#) the optimal sizes of the PV and WG power sources and the batteries are determined by minimizing the system total cost function using linear programming techniques. The total system cost consists of both the initial cost and yearly operation and maintenance costs.

Common disadvantage of the methods described above is that the proposed sizing methodologies do not take into account system design characteristics such as the number of battery chargers, the PV modules tilt angle and the WG installation height, which highly affect both, the resulting energy production and the installation and maintenance costs. Also, the minimization of the system cost function has been implemented either by linearly changing the values of the corresponding decision variables or employing linear programming techniques, resulting in suboptimal solutions and increased computational effort requirements.

In this paper, an alternative methodology for the optimal sizing of stand-alone PV/WG systems is proposed. The purpose of the proposed methodology is to suggest, among a list of commercially available system devices, the optimal number and type of units ensuring that the 20-year round total system cost is minimized subject to the constraint that the load energy requirements are completely covered, resulting in zero load rejection. The 20-year round total system cost is equal to the sum of the respective components capital and maintenance costs. The decision variables included in the optimization process are the number and type of PV modules, WGs and battery chargers, the PV modules tilt angle, the installation height of the WGs and the battery type and nominal capacity. The minimization of the cost (objective) function is implemented employing a genetic algorithms (GA) approach,

which compared to conventional optimization methods, such as dynamic programming and gradient techniques, has the ability to attain the global optimum with relative computational simplicity. GAs have been applied to the design of large power distribution systems (Ramirez-Rosado and Bernal-Agustin, 1998) and the solution of power economic dispatch problems (Li, 1998) because of their ability to handle complex problems with linear or non-linear cost functions both, accurately and efficiently. In the proposed method, GAs are selected because they have shown to be highly applicable to cases of large non-linear systems, where the location of the global optimum is a difficult task. Due to the probabilistic development of solutions, GAs are not restricted by local optima. Thus, given the number of non-linearities that exist in similar problems, GAs appear to be a useful approach.

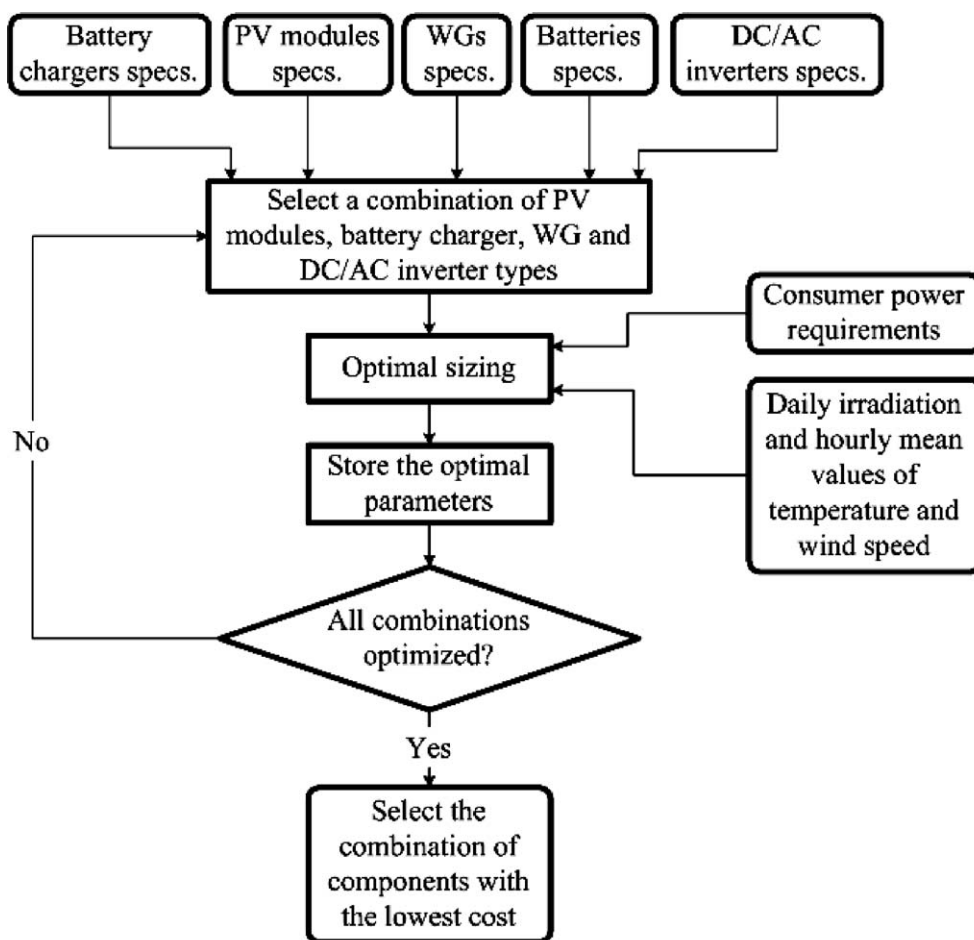


Fig. 2. Flowchart of the proposed optimization methodology.

This paper is organized as follows: the proposed methodology is outlined in Section 2, the hybrid system modeling and operation simulation is described in Section 3, the system cost minimization algorithm using GAs is analyzed in Section 4 and the simulation results are presented in Section 5.

2. The proposed methodology

A general block diagram outlining the proposed methodology is shown in Fig. 2. The optimization algorithm input is fed by a database containing the technical characteristics of commercially available system devices along with their associated per unit capital and maintenance costs. Various types of PV modules and WGs, batteries with different nominal capacities, etc., are stored in the input database, which is implemented in the form of text files for easy maintenance.

The first step of the optimal sizing methodology consists of a system simulation procedure in order to examine whether a system configuration, comprising a certain number of system devices and installation details, fulfills the load power supply requirements during the year. The data used in this case are the daily solar irradiation on horizontal plane, the hourly mean values of ambient temperature and wind speed and the consumer power requirements for an one year time period. The second step of the optimal sizing procedure consists of a method employing GAs, which dynamically searches for the system configuration, which subject to the criterion set in the first step, minimizes the system total cost. For each combination of system device types, the optimal sizing procedure is performed computing the corresponding optimal total system cost and devices configuration. After all device type combinations have been optimally sized as described above, the combination with the lowest cost and the corresponding devices mixture are displayed as the overall optimal system configuration.

3. The PV/WG system modeling and operation simulation

In the proposed method, the system operation is simulated for one year with a time step of 1 h. The power produced by the PV and WG power sources is assumed to be constant during that time period. Therefore, the power generated by the renewable energy sources is numerically equal with the energy generated within this time step.

The current–voltage and power–voltage characteristics of a PV array in each power generation block shown in Fig. 1, which consists of N_P modules connected in parallel, and N_S modules connected in series, are shown in Fig. 3(a). The maximum output power of the PV array on day i ($1 \leq i \leq 365$) and at hour t ($1 \leq t \leq 24$), $P_M^i(t, \beta)$ (W), is calculated using the specifications of the PV module under Standard Test Conditions (STC, cell temperature = 25 °C and solar irradiance = 1 kW/m²), provided by the manufacturer, as well as the ambient temperature and irradiation conditions, according to the following equations:

$$P_M^i(t, \beta) = N_S \cdot N_P \cdot V_{OC}^i(t) \cdot I_{SC}^i(t, \beta) \cdot FF^i(t) \quad (5)$$

$$I_{SC}^i(t, \beta) = \{I_{SC,STC} + K_I[T_C^i(t) - 25^\circ]\} \frac{G^i(t, \beta)}{1000} \quad (6)$$

$$V_{OC}^i(t) = V_{OC,STC} - K_V \cdot T_C^i(t) \quad (7)$$

$$T_C^i(t) = T_A^i(t) + \frac{NCOT - 20^\circ C}{800} G^i(t, \beta) \quad (8)$$

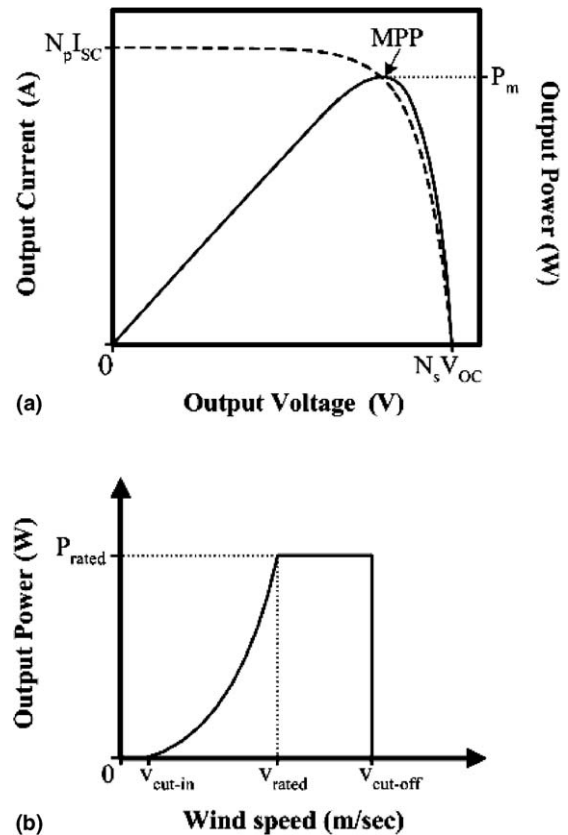


Fig. 3. PV and WG output power characteristics: (a) PV module current–voltage and power–voltage characteristics and (b) WG power versus wind speed characteristic.

where $I_{SC}^i(t, \beta)$ is the PV module short-circuit current (A), $I_{SC,STC}$ is the short-circuit current under STC (A), $G^i(t, \beta)$ is the global irradiance (W/m^2) incident on the PV module placed at tilt angle β ($^\circ$), K_I is the short-circuit current temperature coefficient ($A/^\circ C$), $V_{OC}^i(t)$ is the open-circuit voltage (V), $V_{OC,STC}$ is the open-circuit voltage under STC (V), K_V is the open-circuit voltage temperature coefficient ($V/^\circ C$), $T_A^i(t)$ is the ambient temperature ($^\circ C$), NCOT is the Nominal Cell Operating Temperature ($^\circ C$), provided by the manufacturer and $FF^i(t)$ is the Fill Factor (Markvart, 1994).

The value of $G^i(t, \beta)$ is calculated using the daily solar irradiation on the horizontal plane as analyzed by Lorenzo (1994). The PV modules tilt angle can be selected by the system designer to be either constant during the year, β , or variable with angle β_1 corresponding to the months from January until April (day numbers 1–104) and September until December (day numbers 290–365) and β_2 corresponding to the rest of the year.

The number of PV modules connected in series in the PV array, depends on the battery charger maximum input voltage, V_{DC}^m (V), and the PV modules maximum open-circuit voltage level, V_{OC}^m (V)

$$N_s = \frac{V_{DC}^m}{V_{OC}^m} \quad (9)$$

The PV power actually transferred to the battery bank on day i , $P_{PV}^i(t, \beta)$ (W), is related to the maximum output power of the PV array, $P_M^i(t, \beta)$, through the battery charger conversion factor, n_s , which is defined as

$$n_s \equiv \frac{P_{PV}^i(t, \beta)}{P_M^i(t, \beta)} = n_1 \cdot n_2 \quad (10)$$

where n_1 is the battery charger power electronic interface efficiency, specified by the manufacturer and n_2 is a conversion factor, which depends on the battery charging algorithm and indicates the deviation of the actual PV power generated, from the corresponding maximum power.

In case that the battery charger operates according to the MPPT principle, n_2 is approximately equal to 1, otherwise it differs significantly. An example of the PV array measured output power and the corresponding maximum available power during the bulk-charging phase of a commercial battery charger without MPPT capability, is depicted in Fig. 4. During the bulk-charging phase of this charger, the PV array is directly connected

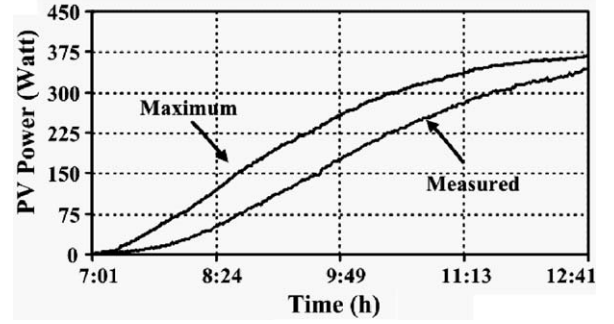


Fig. 4. Deviation of the measured PV array output power from the corresponding maximum power using a PV charger without MPPT function.

to the battery bank. The available solar irradiance during the measurements ranges from 0 to $900 W/m^2$ and the resulting average value of the conversion factor n_2 is approximately 70%.

The number of PV battery chargers, N_{ch}^{PV} , which is also equal with the total number of PV power generation blocks, depends on the total number of PV modules, N_{PV}

$$N_{ch}^{PV} = \frac{N_{PV} \cdot P_{PV}^m}{P_{ch}^m} \quad (11)$$

where P_{ch}^m is the power rating of the selected battery charger (W), and P_{PV}^m is the maximum power of one PV module under STC (W), both specified by their manufacturers.

The diagram of the WG output power versus wind speed is shown in Fig. 3(b). Such a diagram is provided by the manufacturer and it usually indicates the actual power transferred to the battery bank from the WG source, taking into account the effects of both the charger power conversion efficiency and the MPPT operation, if available. Thus, modeling of the WG battery charger characteristics has not been considered in the proposed method. This diagram is input to the optimization algorithm in the form of a lookup table, storing the corresponding output power and wind speed points. During the optimization process, the power transferred to the battery bank, $P_{WG}^i(t, h)$ (W), at hour t of day i , from a WG installed at height h (m), is calculated using the following linear relation:

$$P_{WG}^i(t, h) = P_1 + [v^i(t, h) - v_1] \frac{P_2 - P_1}{v_2 - v_1} \quad (12)$$

where $v^i(t, h)$ is the wind speed (m/s) at height h and (P_1, v_1) , (P_2, v_2) are WG power and wind speed pairs

stored in the lookup table, such that $v_1 < v^i(t, h) < v_2$.

In order to calculate the wind speed, $v^i(t, h)$, at the desired WG installation height, h , which is usually different from the height corresponding to the wind speed input data, the exponential law is used

$$v^i(t, h) = v_{\text{ref}}^i(t) \cdot \left(\frac{h}{h_{\text{ref}}} \right)^a \quad (13)$$

where $v_{\text{ref}}^i(t)$ is the reference (input) wind speed (m/s) measured at height h_{ref} (m) and a is the power law exponent, ranging from 1/7 to 1/4.

The battery bank, with total nominal capacity C_n (A h), is permitted to discharge up to a limit defined by the maximum permissible depth of discharge DOD (%), which is specified by the system designer at the beginning of the optimal sizing process, i.e.

$$C_{\min} = \text{DOD} \cdot C_n \quad (14)$$

where C_{\min} is the minimum permissible battery capacity during discharging (A h).

Depending on the PV and WG energy production and the load power requirements, the battery state of charge is accumulated during the simulation period as follows:

$$C^i(t) = C^i(t-1) + n_B \frac{P_B^i(t)}{V_{\text{BUS}}} \Delta t \quad (15)$$

$$C^i(24) = C^{i+1}(0) \quad (16)$$

where $C^i(t)$, $C^i(t-1)$ is the available battery capacity (A h) at hour t and $t-1$, respectively, of day i , $n_B = 80\%$ is the battery round-trip efficiency during charging and $n_B = 100\%$ during discharging (Borowy and Salameh, 1996), V_{BUS} is the DC bus voltage (V), $P_B^i(t)$ is the battery input/output power (W) [$P_B^i(t) < 0$ during discharging and $P_B^i(t) > 0$ during charging] and Δt is the simulation time step, set to $\Delta t = 1$ h.

The number of batteries connected in series, n_B^S , depends on the nominal DC bus voltage and the nominal voltage of each individual battery, V_B (V), and it is calculated as follows:

$$n_B^S = \frac{V_{\text{BUS}}}{V_B} \quad (17)$$

The battery bank nominal capacity is related with the total number of batteries, N_{BAT} , the number of series connected batteries and the nominal capacity of each battery, C_B (A h), as follows:

$$C_n = \frac{N_{\text{BAT}}}{n_B^S} C_B \quad (18)$$

The modeling equations described above form the simulation algorithm, which is used to verify whether a solution derived by the GA-based cost function minimization procedure fulfills the load power requirements during the whole year. The corresponding flowchart is depicted in Fig. 5. The algorithm input data set consists of the daily solar irradiation on horizontal plane, the hourly mean values of ambient temperature and wind speed, the load power requirements during the year and the specifications of the system devices, while it is executed with a time step of 1 h. Initially, the total power, $P_{\text{re}}^i(t)$ (W), transferred to the battery bank from the PV and WG power sources during day i ($1 \leq i \leq 365$) and hour t ($1 \leq t \leq 24$) is calculated as follows:

$$P_{\text{re}}^i(t) = N_{\text{PV}} \cdot P_{\text{PV}}^i(t, \beta) + N_{\text{WG}} \cdot P_{\text{WG}}^i(t, h) \quad (19)$$

where h is the WG installation height, N_{PV} is the total number of PV modules and N_{WG} is total the number of WGs. The PV modules tilt angle β is either constant during the year, or takes the values β_1, β_2 as described above.

Then, the DC/AC inverter input power, $P_L^i(t)$ (W), is calculated using the corresponding load power requirements, as follows:

$$P_L^i(t) = \frac{P_{\text{load}}^i(t)}{n_i} \quad (20)$$

where $P_{\text{load}}^i(t)$ (W) is the power consumed by the load at hour t of day i , defined at the beginning of the optimal sizing process and n_i is the DC/AC converter efficiency (%), specified by the manufacturer.

According to the above power production and load consumption calculations, the resulting battery capacity is calculated

- If $P_{\text{re}}^i(t) = P_L^i(t)$ then the battery capacity remains unchanged.
- If $P_{\text{re}}^i(t) > P_L^i(t)$ then the power surplus $P_B^i(t) = P_{\text{re}}^i(t) - P_L^i(t)$ is used to charge the battery bank and the new battery capacity is calculated using Eq. (15). In case that the battery SOC reaches the 100% SOC limit then the remainder of the available power is not used.
- If $P_{\text{re}}^i(t) < P_L^i(t)$ then the power deficit $P_B^i(t) = P_{\text{re}}^i(t) - P_L^i(t)$ required to cover the load energy requirements is supplied by the battery bank and the new battery capacity is calculated using Eq. (15).

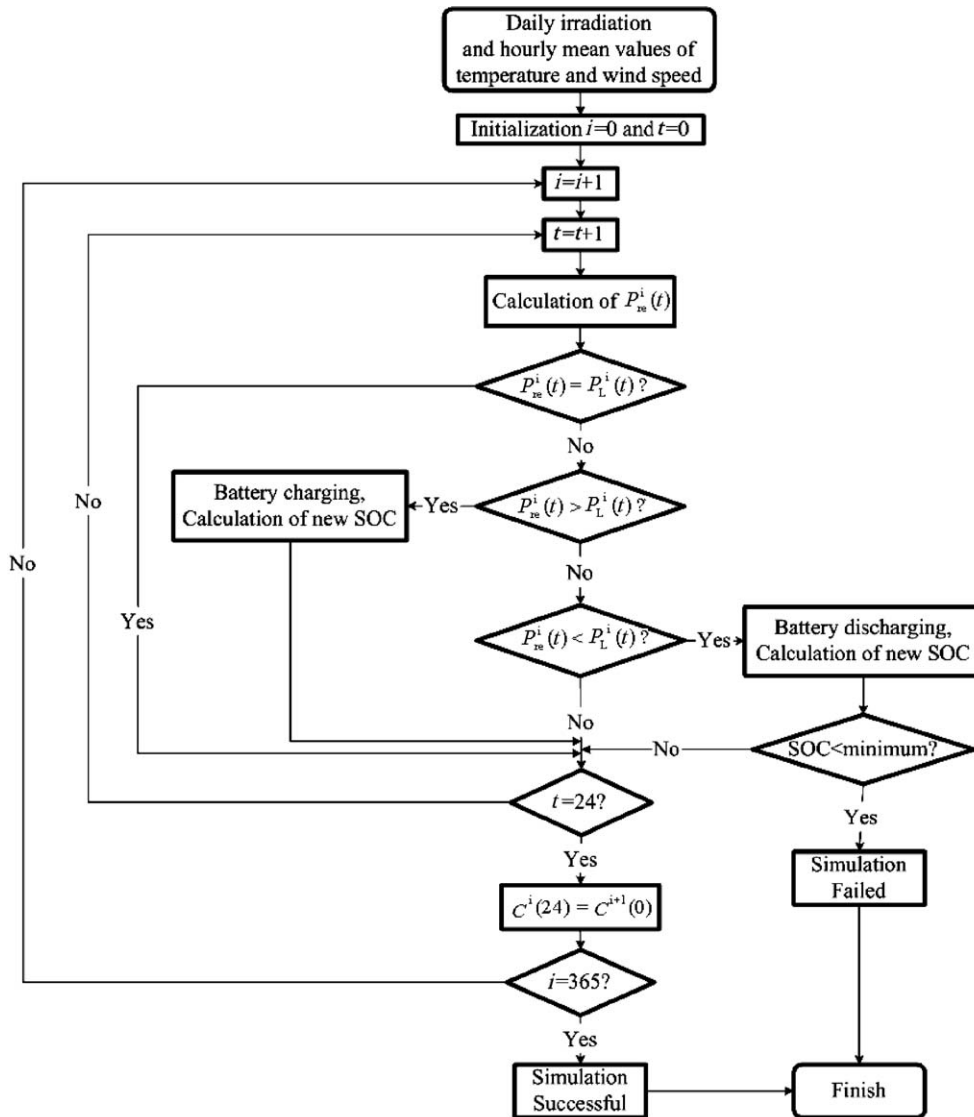


Fig. 5. Flowchart of the algorithm simulating the system operation.

The above steps are repeated until either the simulation time period finishes, at day number 365 and the 24th hour, indicating successful system operation, or the battery bank is discharged below the lowest permissible limit defined by Eq. (14). In such case, the system operation is considered to fail and the corresponding configuration is rejected, since it does not guarantee reliable power supply of the load.

4. System cost minimization algorithm using GAs

Genetic algorithms are adaptive search and optimization approaches that work mimicking the prin-

ciples of natural genetics. GAs are very different from traditional search and optimization methods used in engineering design problems. Fundamental ideas of genetics in biology are borrowed and used artificially to construct search algorithms that are robust and require minimal problem information.

A typical constrained, single variable optimization problem can be outlined as follows:

$$\text{Maximise}_x f(x) \quad (21)$$

subject to the constraint : $x_{\min} \leq x \leq x_{\max}$

For the solution of such a problem with GAs the variable x is typically coded in some string struc-

tures. Binary-coded or floating point strings can also be used, while the length of the string is usually determined according to the accuracy of the solution desired. The GA, as any evolution procedure for a particular problem, must have the following components (Michalewicz, 1994):

- A generic representation for potential solutions to the problem, similar to the system modeling presented in the previous section.
- A way to create an initial population of potential solutions.
- An evaluation function that plays the role of the environment, rating solutions in terms of their “fitness” and
- Genetic operators (such as crossover and mutation) that alter the composition of children.

In the proposed method, the GA optimal sizing methodology outputs the optimum number of WGs, PV modules, batteries and PV battery chargers, along with the optimum PV modules tilt angle and WGs installation height, comprising the set of decision variables, such that the 20-year round total system cost function, $J(\mathbf{x})$ (€), is minimized. The total system cost function is equal to the sum of the total capital, $C_c(\mathbf{x})$ (€), and maintenance cost, $C_m(\mathbf{x})$ (€), functions

$$\min_{\mathbf{x}}\{J(\mathbf{x})\} = \min_{\mathbf{x}}\{C_c(\mathbf{x}) + C_m(\mathbf{x})\} \quad (22)$$

where \mathbf{x} is the vector of the decision variables listed above.

Thus, multi-objective optimization is achieved by minimizing the total cost function consisting of the sum of the individual system devices capital and 20-year round maintenance costs

$$\begin{aligned} J(N_{PV}, N_{WG}, N_{BAT}, N_{ch}^{PV}, h, \beta) &= N_{PV} \cdot (C_{PV} + 20 \cdot M_{PV}) + N_{WG} \cdot (C_{WG} \\ &+ 20 \cdot M_{WG} + h \cdot C_h + 20 \cdot h \cdot C_{hm}) \\ &+ N_{BAT} \cdot [C_{BAT} + y_{BAT} \cdot C_{BAT} \\ &+ (20 - y_{BAT} - 1) \cdot M_{BAT}] + N_{ch}^{PV} \cdot C_{ch}^{PV} \cdot (y_{ch}^{PV} + 1) \\ &+ N_{ch}^{PV} \cdot M_{ch}^{PV} \cdot (20 - y_{ch}^{PV} - 1) + C_{INV} \cdot (y_{INV} + 1) \\ &+ M_{INV} \cdot (20 - y_{INV} - 1) \end{aligned} \quad (23)$$

or, equivalently, by maximizing the GA fitness function

$$\begin{aligned} F(N_{PV}, N_{WG}, N_{BAT}, N_{ch}^{PV}, h, \beta) &= \begin{cases} C_{\max} - J(N_{PV}, N_{WG}, N_{BAT}, N_{ch}^{PV}, h, \beta), \\ \text{if } C_{\max} - J(N_{PV}, N_{WG}, N_{BAT}, N_{ch}^{PV}, h, \beta) > 0 \\ 0, \text{ otherwise} \end{cases} \end{aligned} \quad (24)$$

subject to the constraints

$$N_{PV} \geq 0 \quad (25)$$

$$N_{WG} \geq 0 \quad (26)$$

$$N_{BAT} \geq 0 \quad (27)$$

$$N_{ch}^{PV} \geq 0 \quad (28)$$

$$h_{low} \leq h \leq h_{high} \quad (29)$$

$$\left[\begin{array}{l} 0^\circ \leq \beta \leq 90^\circ \text{ or} \\ 0^\circ \leq \beta_1 \leq 90^\circ \text{ and } 0^\circ \leq \beta_2 \leq 90^\circ \end{array} \right] \quad (30)$$

$$\left[\begin{array}{l} \text{Simulation}(N_{PV}, N_{WG}, N_{BAT}, N_{ch}^{PV}, h, \beta) = \text{Successful or} \\ \text{Simulation}(N_{PV}, N_{WG}, N_{BAT}, N_{ch}^{PV}, h, \beta_1, \beta_2) = \text{Successful} \end{array} \right] \quad (31)$$

where h_{low} , h_{high} are the WG tower lower and upper height limits (m), respectively, specified by the WG manufacturer, C_{PV} , C_{WG} , and C_{BAT} are the capital costs (€) of one PV module, WG and battery, respectively, M_{PV} , M_{WG} , and M_{BAT} are the maintenance costs per year (€/year) of one PV module, WG and battery, respectively, C_h is the WG tower capital cost per meter (€/m), C_{hm} is the WG tower maintenance cost per meter and year (€/m/year), C_{ch}^{PV} is the capital cost of one PV battery charger (€), y_{ch}^{PV} , y_{INV} are the expected numbers of PV battery charger and DC/AC inverter replacements during the 20-year system lifetime and it is equal to the system lifetime (20 years) divided by the Mean Time Between Failures (MTBF) of power electronic converters (Holtz et al., 1994), C_{INV} is the capital cost of the DC/AC inverter, (€), y_{BAT} is the expected number of battery replacements during the 20-year system operation, because of limited battery lifetime, M_{ch}^{PV} , M_{INV} maintenance costs per year (€/year) of one PV battery charger and DC/AC inverter, respectively and C_{\max} is the absolute minimum of function $J(\mathbf{x})$ calculated at each generation, (€).

The Simulation(·) function performs the system simulation described in Section 3, in order to verify that the examined system configuration fulfils the uninterrupted power supply requirement of the load during the whole year.

Real-Coded GA techniques are introduced for the solution of the optimization problem based on the

mechanism of natural selection and natural genetics. Each chromosome consists of five genes in the form: $[N_{PV}|N_{WG}|N_{BAT}|h|\beta]$. In case that the PV modules inclination changes seasonally, then six genes are used in the optimization algorithm and each chromosome is of the form: $[N_{PV}|N_{WG}|N_{BAT}|h|\beta_1|\beta_2]$. The number of PV battery chargers has not been incorporated into the chromosome configuration in order to reduce the algorithm complexity, since, as expressed in Eq. (11), it depends on the PV array power rating, which in turn depends on the number of PV modules, N_{PV} . However, the number of PV battery chargers affects the total system cost, thus the associated cost has been included in the GA fitness function, as expressed in Eq. (24).

The flowchart of the GA optimization process is depicted in Fig. 6. An initial population of 30 chromosomes, comprising the 1st generation, is generated randomly and the constraints described by inequalities (25)–(31) are evaluated for each chromosome. If any of the initial population chromosomes violates the problem constraints then it is replaced by a new chromosome, which is generated randomly and fulfils these constraints.

The first step of the algorithm iteration is the fitness function evaluation for each chromosome of the corresponding population. If any of the resulting fitness function values is lower than the lowest value obtained at the previous iterations then this value is considered to be the optimal solution of the minimization problem and the corresponding chromosome consists of the hybrid system optimal operational parameter values. This optimal solution is replaced by better solutions, if any, produced in subsequent GA generations during the program evolution.

In order to select the chromosomes, which will be subject to the crossover and mutation operations in order to produce the next generation population, a selection operation is applied based on the roulette wheel method (Michalewicz, 1994).

The crossover mechanism uses the following three operators:

Simple Crossover, (SC) with initial probability $p_{sc} = 10\%$.

Simple Arithmetical Crossover, (SAC) with initial probability $p_{sac} = 10\%$.

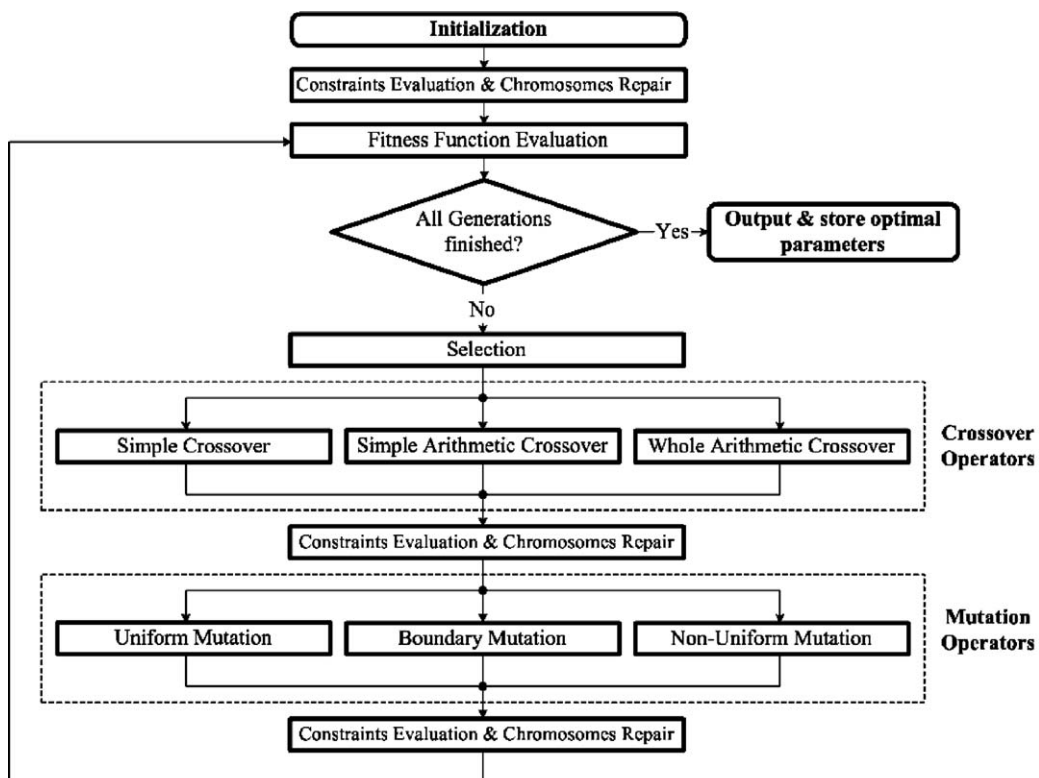


Fig. 6. The GA optimization process.

Whole Arithmetical Crossover (WAC) with initial probability $p_{\text{wac}} = 10\%$. If the chromosomes $\mathbf{c}_1 = [u_1 \dots u_m]$ and $\mathbf{c}_2 = [w_1 \dots w_m]$ are to be crossed then the resulting offspring consists of $\mathbf{c}'_1 = a_{\text{wac}} \cdot \mathbf{c}_1 + (1 - a_{\text{wac}}) \cdot \mathbf{c}_2$ and $\mathbf{c}'_2 = (1 - a_{\text{wac}}) \cdot \mathbf{c}_1 + a_{\text{wac}} \cdot \mathbf{c}_2$. The parameter a_{wac} is set equal to 0.75.

For each chromosome selected for crossover, a random number r ($0 \leq r \leq 1$) is generated. Depending on the value of r , one of the previous crossover operators is applied

- $r < p_{\text{sc}}$ then this chromosome is selected for SC,
- $p_{\text{sc}} \leq r < (p_{\text{sc}} + p_{\text{sac}})$ then the SAC operator is applied,
- $(p_{\text{sc}} + p_{\text{sac}}) \leq r < (p_{\text{sc}} + p_{\text{sac}} + p_{\text{wac}})$ then the chromosome is selected for WAC and finally,
- $r \geq (p_{\text{sc}} + p_{\text{sac}} + p_{\text{wac}})$ then none of the three crossover operators is applied.

Next, the selected chromosomes are subject to the mutation mechanism, which is performed using the following three operators:

Uniform Mutation, (UM). During UM a gene is randomly selected and it is assigned a new value, randomly selected from the corresponding range of values which fulfill the optimization problem constraints. This range of values is calculated for the selected gene, considering the values of the other genes within the chromosome constant. The mutation probability, p_{um} , is 10%.

Boundary mutation, (BM). The boundary mutation probability, p_{bm} , is 3%.

Non-uniform mutation, (NUM). The non-uniform mutation probability, p_{num} , is 35%, in order

to enhance the fine local tuning capability during the optimization process.

For each chromosome a random number, r , ($0 \leq r \leq 1$) is generated

- $r < p_{\text{um}}$ then this chromosome is selected for UM,
- $p_{\text{um}} \leq r < (p_{\text{bm}} + p_{\text{um}})$ then the BM operator is applied,
- $(p_{\text{bm}} + p_{\text{um}}) \leq r < (p_{\text{bm}} + p_{\text{um}} + p_{\text{num}})$ then the chromosome is selected for NUM and finally,
- $r \geq (p_{\text{bm}} + p_{\text{um}} + p_{\text{num}})$ then none of the three mutation operators is applied.

In case that the application of any of the crossover or mutation operators described above, results in a chromosome which does not satisfy the optimization problem constraints, then a “repair” procedure is performed and that chromosome is replaced by the corresponding parent. In case of SC operation, where each new chromosome is generated by two parents, then the chromosome is replaced by the parent with the best fitness function value.

The GA optimization process described above is repeated until a predefined number of population generations have been evaluated.

5. Simulation results

The proposed method has been applied to the design of a stand-alone hybrid PV/WG system in order to power supply a residential household located in the area of the Technical University of Crete (TUC) with geographical coordinates defined as

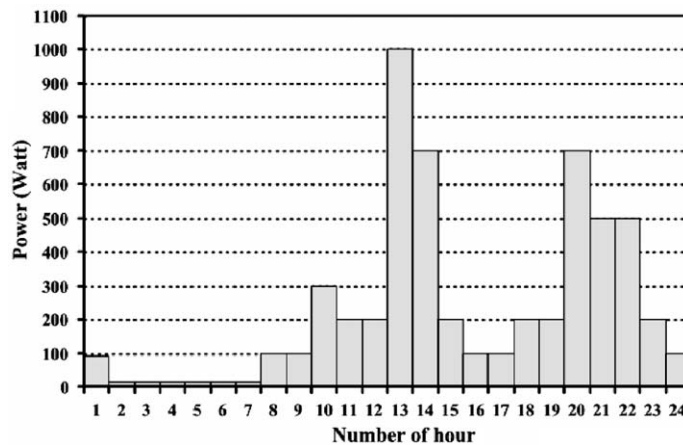


Fig. 7. Distribution of the consumer power requirements during the day.

Latitude: 35.53° (35°31'48"N),
 Longitude: 24.06° (24°03'35"E) and
 Altitude: 150 m (approx.) above sea level.

The distribution of the consumer power requirements during a day (Lazou and Papatsoris, 2000) is shown in Fig. 7. It is assumed that the user appliances are energy efficient and energy saving load management strategies are applied, which are common practices in renewable energy applications. The daily solar irradiation on horizontal plane, as well as the hourly mean values of ambient temperature and wind speed, plotted in Fig. 8 during the

year 2003, were recorded using a properly developed data-acquisition system installed at the TUC campus.

The technical characteristics and the related capital and maintenance costs of the hybrid system devices, which are input to the optimal sizing procedure, are shown in Tables 1–5. The installation cost has been included in the capital cost of the devices, while the maintenance cost of each unit per year has been set at 1% of the corresponding capital cost. The MTBF of the battery chargers and DC/AC inverter has been set equal to 40,000 h. The expected battery lifetime has been set at 3 years resulting in $y_{\text{BAT}} = 6$.

The optimal sizing results, consisting of both the devices type and their number, for each combination of system devices included in Tables 1–5, are shown in Table 6. The overall optimal solution is combination #5, resulting in a 20-year round system cost of 37,524 €. It is noteworthy that a PV charger with MPPT capability has been selected in the optimal solution, although of higher per unit cost compared to the other PV charger option as shown in Table 5, since it achieves better exploitation of the available PV power. The corresponding battery bank has an optimal total nominal capacity of 920 A h and the available capacity variation during the year is depicted in Fig. 9. The maximum depth of discharge is approximately 63.7%, thus indicating the system capability to supply reliably the consumer load. Also, the variation of the system total cost (fitness function) during the GA optimization procedure of Combination #5 is shown in Fig. 10. It can be noted that a near optimal solution was derived during the early stages of the GA generations evolution. The CPU time required for the evolution of the 721 generations in the diagram of Fig. 10 is approximately 3 min (Pentium IV, 2.6 GHz).

The optimal sizing results, for each combination of system devices included in Tables 1–5, in case that the power source consists either only of WGs or only of PV modules are tabulated in Tables 7 and 8, respectively. It is observed that in both cases the overall optimal solutions, i.e. combinations #1 and #5, respectively, result in substantially higher total system cost compared to the hybrid PV/WG system design. Also the PV-only system results in approximately double total cost compared to the WG-only system because of the much higher per unit capital cost of PV modules.

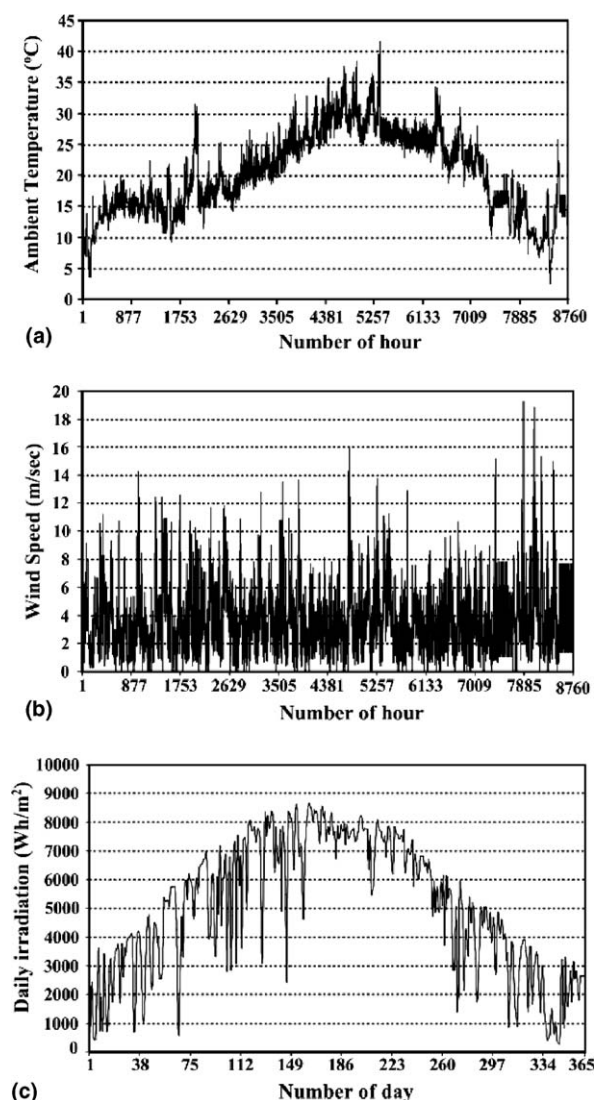


Fig. 8. Hourly mean values during the year 2003 of meteorological conditions: (a) ambient temperature, (b) wind speed and (c) daily irradiation on horizontal plane.

Table 1
Batteries specifications

Type	Nominal capacity (A h)	Voltage (V)	DOD (%)	Capital cost (€)	Maintenance cost per year (€/year)
1	230	12	80	264	2.64
2	100	12	80	126	1.26

Table 2
WGs specifications

Type	Power rating (W)	h_{low} (m)	h_{high} (m)	Capital cost (€)	Maintenance cost per year (€/year)	Tower capital cost per meter (€/m)	Tower maintenance cost per year and per meter (€/year/m)
1	1000	8	15	1681	16.81	55	0.55
2	400	8	15	512	11.9	11	0.11

Table 3
PV modules specifications

Type	V_{oc} (V)	I_{sc} (A)	V_{max} (V)	I_{max} (A)	P_{max} (W)	NCOT (°C)	Capital cost (€)	Maintenance cost per year (€/year)
1	21.6	3.48	17.3	3.18	55	43	265.81	2.66
2	21	7.22	17	6.47	110	43	519.14	5.19

Table 4
DC/AC inverter specifications

Type	Efficiency (%)	Power rating (W)	Capital cost (€)	Maintenance cost per year (€/year)
1	80	1500	1942.0	19.42

Table 5
PV battery chargers specifications

Type	n_1 (%)	n_2 (%)	Power rating (W)	Capital cost (€)	Maintenance cost per year (€/year)
1	95	100	300	200.0	2.0
2	95	70	240	94.0	0.94

A remark concerning the tilt angles β_1 and β_2 tabulated in Tables 6 and 8, is that the tilt angle values corresponding to the winter period, β_1 , are sometimes lower than the relevant ones for the summer period, β_2 . This is due to the solar irradiation profile of the site under consideration, exhibiting prolonged cloudy intervals during the winter, resulting in low optimal β_1 tilt angle values, since the main component of the global irradiation under cloudy conditions is the diffused radiation, which is maximized at low tilt angles. Also, the tilt angle β_2 values are sometimes higher compared to the typical angle values calculated using the latitude of the installation site. For example, $\beta_2 = 73^\circ$ in the combination of row #5 in Table 6 and $\beta_2 = 79^\circ$ in the combination of row #3 in Table 8, etc., while typical

installation procedures impose tilt angles less than 60° for the site under consideration. These β_2 tilt angle values, which minimize the system cost, result in case that the system components optimal mixture is such that PV energy surplus is produced during the summer period, thus the zero load rejection constraint is satisfied without requiring further reduction of the β_2 angle value.

In all preceding cases, the proposed algorithm convergence to the global optimum solution has been verified, using a properly developed simulation program, by linearly changing the values of all decision variables included in the optimization process and calculating the corresponding 20-year round system cost. This procedure is repeated for each combination of system components types. The

Table 6
Hybrid system optimal sizing results

Combination	Device type					Number of PVs	Number of WGs	Number of batteries	WG height (m)	Number of PV Chargers	PV tilt β_1 (°)	PV tilt β_2 (°)	Total cost (€)
	WG	PV	Charger	Inverter	Battery								
1	1	1	1	1	1	19	3	6	15	4	50	44	40497.29
2	1	1	1	1	2	22	3	10	15	4	53	12	39144.08
3	1	1	2	1	1	17	3	8	15	4	54	28	41440.38
4	1	1	2	1	2	20	3	14	15	5	54	54	40400.16
5	1	2	1	1	1	11	3	4	15	4	42	73	37524.83
6	1	2	1	1	2	11	3	10	15	4	46	60	38979.35
7	1	2	2	1	1	9	3	8	14	5	45	55	41910.67
8	1	2	2	1	2	12	3	12	15	6	52	21	40183.68
9	2	1	1	1	1	22	16	9	15	4	50	32	53247.56
10	2	1	1	1	2	29	14	17	15	6	51	17	53975.95
11	2	1	2	1	1	30	16	9	15	7	52	72	55068.04
12	2	1	2	1	2	29	16	20	15	7	51	78	55775.79
13	2	2	1	1	1	13	14	9	15	5	58	26	53462.76
14	2	2	1	1	2	14	16	16	15	6	50	19	54444.93
15	2	2	2	1	1	15	16	9	15	7	53	49	54843.40
16	2	2	2	1	2	15	17	19	15	7	52	59	55919.74

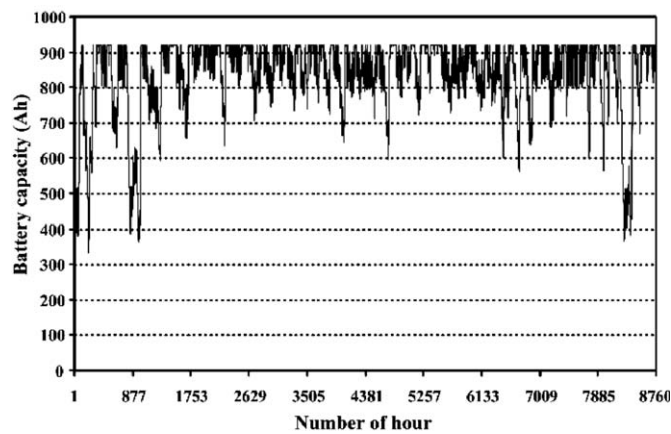


Fig. 9. Simulated available battery capacity corresponding to the optimal solution, during the year.

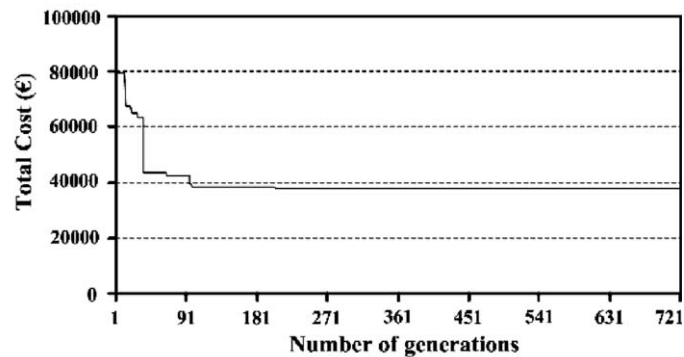


Fig. 10. The system total cost during the GA optimization.

Table 7
Optimal sizing results for WG-only power source

Combination	Device type			Number of WGs	Number of batteries	WG height (m)	Total cost (€)
	WG	Inverter	Battery				
1	1	1	1	5	10	15	43860.50
2	1	1	2	5	24	15	46598.42
3	2	1	1	31	21	15	142753.22
4	2	1	2	31	48	15	146346.74

Table 8
Optimal sizing results for PV-only power source

Combination	Device type				Number of PVs	Number of batteries	Number of PV chargers	PV tilt β_1 (°)	PV tilt β_2 (°)	Total cost (€)
	PV	Chargers	Inverter	Battery						
1	1	1	1	1	57	26	11	15	11	88453.02
2	1	1	1	2	58	59	11	12	20	92836.10
3	1	2	1	1	73	28	17	31	79	94220.92
4	1	2	1	2	75	62	18	24	49	98337.56
5	2	1	1	1	29	26	11	12	54	88337.69
6	2	1	1	2	31	57	12	6	64	92880.97
7	2	2	1	1	36	28	17	30	47	93362.81
8	2	2	1	2	39	61	18	19	21	97812.03

resulting optimal solution, for each combination of system components types, is equal to the solution derived using the proposed GA optimization method, in terms of both the total system cost and the values of the decision variables, thus proving the GA optimization procedure convergence to the global optimum solution. However, the CPU time required by the simulation program to derive the optimal solution for each combination of system components types is approximately 20 h, while using the proposed method the corresponding time required is approximately 3 min.

6. Conclusions

The major aspects in the design of PV and/or WG power generation systems are (a) the reliable power supply of the consumer under varying atmospheric conditions and (b) the corresponding total system cost. Past proposed PV/WG system sizing methods suffer the disadvantage of not taking into account system design characteristics such as the number of battery chargers, the PV modules tilt angle and the WG installation height, which highly affect both the resulting energy production and the installation and maintenance costs. Also, in the existing literature, the minimization of the system cost function is implemented either by linearly changing the number of the corresponding decision

variables or employing linear programming techniques, resulting in suboptimal solutions and increased computational effort requirements.

In this paper, a methodology for the optimal sizing of hybrid, stand-alone PV/WG systems, has been presented. The purpose of the proposed methodology is to support the selection, among a list of commercially available system devices, the optimal number and type of PV modules, WGs and PV battery chargers, the PV modules tilt angle, the installation height of the WGs and the battery type and nominal capacity. The optimal number and type of each system component is calculated such that the 20-year round total system cost is minimized subject to the constraint that the load power requirements are completely covered, thus resulting in zero load rejection. The 20-year round total system cost is equal to the sum of the respective components capital and maintenance costs. The cost (objective) function minimization is implemented using genetic algorithms, which compared to conventional optimization methods, such as dynamic programming and gradient techniques, have the ability to attain the global optimum with relative computational simplicity. The proposed method has been applied to the design of a power generation system in order to supply a residential household. The simulation results verify that hybrid PV/WG systems result in lower system cost compared to

cases where either exclusively WG or exclusively PV sources are used.

References

- Bagul, A.D., Salameh, Z.M., Borowy, B., 1996. Sizing of a stand-alone hybrid wind-photovoltaic system using a three-event probability density approximation. *Solar Energy* 56 (4), 323–335.
- Borowy, B.S., Salameh, Z.M., 1996. Methodology for optimally sizing the combination of a battery bank and PV array in a wind/PV hybrid system. *IEEE Transactions on Energy Conversion* 11 (2), 367–373.
- Chedid, R., Rahman, S., 1997. Unit sizing and control of hybrid wind-solar power systems. *IEEE Transactions on Energy Conversion* 12 (1), 79–85.
- De Broe, A.M., Drouilhet, S., Gevorgian, V., 1999. A peak power tracker for small wind turbines in battery charging applications. *IEEE Transactions on Energy Conversion* 14 (4), 1630–1635.
- Holtz, J., Lotzkat, W., Stadtfeld, S., 1994. Controlled AC drives with ride-through capability at power interruption. *IEEE Transactions on Industry Applications* 30 (5), 1275–1283.
- Kellogg, W.D., Nehrir, M.H., Venkataramanan, G., Gerez, V., 1998. Generation unit sizing and cost analysis for stand-alone wind, photovoltaic and hybrid wind/PV systems. *IEEE Transactions on Energy Conversion* 13 (1), 70–75.
- Lazou, A., Papatsoris, A., 2000. The economics of photovoltaic stand-alone residential households: a case study for various European and Mediterranean locations. *Solar Energy Materials & Solar Cells* 62, 411–427.
- Li, F., 1998. A comparison of genetic algorithms with conventional techniques on a spectrum of power economic dispatch problems. *Expert Systems with Applications* 15, 133–142.
- Lorenzo, E., 1994. *Solar Electricity: Engineering of Photovoltaic Systems*, first ed. Progensa.
- Maghraby, H.A.M., Shwehdi, M.H., Al-Bassam, G.K., 2002. Probabilistic assessment of photovoltaic (PV) generation systems. *IEEE Transactions on Power Systems* 17 (1), 205–208.
- Markvart, T., 1994. *Solar Electricity*, first ed. Wiley.
- Markvart, T., 1996. Sizing of hybrid photovoltaic-wind energy systems. *Solar Energy* 57 (4), 277–281.
- Michalewicz, Z., 1994. *Genetic algorithms + data structures = evolution programs*, second ed. Springer-Verlag.
- Ramirez-Rosado, I.J., Bernal-Agustin, J.L., 1998. Genetic algorithms applied to the design of large power distribution systems. *IEEE Transactions on Power Systems* 13 (2), 696–703.
- Shrestha, G.B., Goel, L., 1998. A study on optimal sizing of stand-alone photovoltaic stations. *IEEE Transactions on Energy Conversion* 13 (4), 373–378.
- Yokoyama, R., Ito, K., Yuasa, Y., 1994. Multiobjective optimal unit sizing hybrid power generation systems utilizing photovoltaic and wind energy. *Transactions of the ASME: Journal of Solar Energy Engineering* 116, 167–173.